

Proteomic Analysis Reveals That the Rab GTPase RabE1c Is Involved in the Degradation of the Peroxisomal Protein Receptor PEX7 (Peroxin 7)*

Received for publication, November 19, 2012, and in revised form, December 30, 2012. Published, JBC Papers in Press, January 7, 2013, DOI 10.1074/jbc.M112.438143

Songkui Cui^{‡§}, Yoichiro Fukao[¶], Shoji Mano^{‡§}, Kenji Yamada^{‡§}, Makoto Hayashi^{‡§}, and Mikio Nishimura^{‡§1}

From the [‡]Department of Cell Biology, National Institute for Basic Biology, Okazaki 444-8585, Japan, the [§]Department of Basic Biology, School of Life Science, Graduate University for Advanced Studies, Okazaki 444-8585, Japan, and the [¶]Plant Global Educational Project, Nara Institute of Science and Technology, Ikoma 630-0192, Japan

Background: PEX7 mediates the import of peroxisomal proteins from the cytosol.

Results: The small GTPase RabE1c binds PEX7 on peroxisomes and mediates its degradation.

Conclusion: RabE1c is responsible for PEX7 dislocation/degradation on the peroxisome membrane.

Significance: By proteomic analysis, we identified a novel protein that regulates PEX7 function and revealed a crucial mechanism for PEX7 translocation from the peroxisome membrane.

The biogenesis of peroxisomes is mediated by peroxins (PEXs). PEX7 is a cytosolic receptor that imports peroxisomal targeting signal type 2 (PTS2)-containing proteins. Although PEX7 is important for protein transport, the mechanisms that mediate its function are unknown. In this study, we performed proteomic analysis to identify PEX7-binding proteins using transgenic *Arabidopsis* expressing green fluorescent protein (GFP)-tagged PEX7. Our analysis identified RabE1c, a small GTPase, as a PEX7 binding partner. *In vivo* analysis revealed that GTP-bound RabE1c binds to PEX7 and that a subset of RabE1c localizes to peroxisomes and interacts with PEX7 on the peroxisome membrane. Unlike endogenous PEX7, which is predominantly localized to the cytosol, GFP-PEX7 accumulates abnormally on the peroxisomal membrane and induces degradation of endogenous PEX7, concomitant with a reduction in import of PTS2-containing proteins and decreased peroxisomal β -oxidation activity. Thus, GFP-PEX7 on the peroxisomal membrane exerts a dominant negative effect. Mutation of RabE1c restored endogenous PEX7 protein expression and import of PTS2-containing proteins as well as peroxisomal β -oxidation activity. Treatment with proteasome inhibitors also restored endogenous PEX7 protein levels in GFP-PEX7-expressing seedlings. Based on these findings, we conclude that RabE1c binds PEX7 and facilitates PEX7 degradation in the presence of immobile GFP-PEX7 accumulated at the membrane.

Because peroxisomes lack their own genome, all of their constituent proteins are encoded in the nuclear genome and translated on cytosolic ribosomes before being imported into peroxisomes. Two types of peroxisomal targeting signals, type 1

(PTS1)² and type 2 (PTS2), have been identified in peroxisomal matrix enzymes. PTS1 signals are found at C termini and consist of tripeptide variants (1), whereas PTS2 signals consist of nonapeptides found in cleavable N-terminal presequences (2). About one-fifth of peroxisomal enzymes contain PTS2, including several proteins involved in fatty acid metabolism (e.g. 3-ketoacyl-CoA thiolase, citrate synthase, malate dehydrogenase, and long-chain acyl-CoA oxidase) (2–5). These PTS2-containing proteins are synthesized as precursors in the cytosol before import into the peroxisomes. Upon import, the signal peptides are cleaved by the PTS2-processing enzyme, DEG15 endopeptidase (6).

Studies in different organisms have revealed two soluble import receptors: PEX5 for PTS1 and PEX7 for PTS2 (7, 8). PEX5 and PEX7 interact with each other to facilitate peroxisomal protein import. Mammals possess two isoforms of PEX5, only the longer of which (PEX5L) binds to PEX7 (9, 10). In *Arabidopsis*, which has a single PEX5 isoform, yeast two-hybrid and bimolecular fluorescence complementation (BiFC) assays have demonstrated that PEX7 directly binds to PEX5 in the cytosol. The middle region of PEX7, which contains the WD40 repeat domain, is necessary and sufficient for the interaction with PEX5 (11–13). An *Arabidopsis pex5* mutant that lacks PEX7 binding activity is defective in PTS2-containing protein transport, demonstrating that the import of PTS2-containing proteins is dependent on PEX7 binding to PEX5 (8). In *Saccharomyces cerevisiae*, PTS2-containing protein transport requires both PEX7 and its auxiliary proteins, PEX18 and PEX21, instead of PEX5 (14). In *Neurospora crassa*, *Yarrowia lipolytica*, and *Pichia pastoris*, PEX18 and PEX21 are replaced by a single PEX7 docking protein, PEX20 (15, 16). These auxiliary proteins and mammalian PEX5L share common motif sequences involved in PEX7 interactions. The lack of these auxiliary pro-

* This work was supported by Grant-in-aid for Scientific Research on Innovative Areas 22120007 from the Ministry of Education, Science, Sports, and Culture of Japan (to M. N.).

¹ To whom correspondence should be addressed: Dept. of Cell Biology, National Institute for Basic Biology, 38 Nishigonaka, Myodaiji, Okazaki 444-8585, Aichi, Japan. Tel.: 564-55-7500; Fax: 564-53-7400; E-mail: mikosome@nibb.ac.jp.

² The abbreviations used are: PTS, peroxisomal targeting signal; 2,4-D, 2,4-dichlorophenoxyacetic acid; 2,4-DB, 2,4-dichlorophenoxybutyric acid; BiFC, bimolecular fluorescence complementation; CAT, catalase; DDM, *n*-dodecyl β -D-maltoside; PEX, peroxin; cYFP and nYFP, C-terminal and N-terminal YFP, respectively.

teins in plants and mammals suggests that they may have been functionally replaced by PEX5 in these organisms.

The translocation machinery of PEX5 has been studied in detail. The PEX5-PEX7 complex is recruited with its cargo to the peroxisomal membrane, where it binds to the peroxisomal docking proteins PEX13 and PEX14 (11, 17). After the cargo is released at the peroxisomal membrane, free PEX5 is ubiquitinated by machinery including the E2 enzyme PEX4 (18), the PEX4-interacting protein PEX22 (19), and the RING finger E3 enzymes PEX2, PEX10, and PEX12 (20, 21). Ubiquitination acts as a signal for the release of PEX5 from peroxisomes, and the releasing process is supported by the AAA ATPases PEX1 and PEX6 (22). Monoubiquitinated PEX5 then moves from the peroxisome to the cytosol, where it engages in the next round of import, whereas polyubiquitinated PEX5 is targeted to the 26 S proteasome for degradation (23, 24). In contrast to PEX5, little is known about the import and dislocation machinery of PEX7.

In order to identify PEX7-binding proteins, we performed a proteomic analysis of *Arabidopsis* expressing GFP-PEX7. In this analysis, we identified the small GTPase protein RabE1c and confirmed its interaction with PEX7 *in vivo*. In addition, we showed that RabE1c is part of the PEX7 dislocation machinery and is involved in PEX7 degradation. Our proteomic study of GFP-PEX7-expressing plants provides novel insight into the mechanism of PEX7 import into and dislocation from peroxisomes.

EXPERIMENTAL PROCEDURES

Plant Materials and Growth Conditions—*Arabidopsis thaliana* (Columbia accession) wild type, *rabe1c* mutant, *pex7i* knockdown, and transgenic GFP-PTS1, GFP-PEX16, GFP-PEX7 plants were used. The *pex7i* knockdown and GFP-PTS1, GFP-PEX16, and GFP-PEX7 transgenic plants were described previously (12, 13, 25, 26). A *rabe1c* knock-out mutant (SALK_055451) was obtained from the Arabidopsis Biological Resource Center. The presence of a T-DNA insertion was confirmed by PCR with a RabE1c-specific primer conjugated with *attB1* at the 5' end (5'-AAAAAGCAGGCTCAATGGCTGCTCCACCTGCT-3') and the T-DNA-specific primer SALK LBa1 (5'-TGGTTCACGTAGTGGGCCATCG-3'). The *rabe1c* mutant was crossed with GFP-PEX7 to generate a GFP-PEX7/*rabe1c* transgenic plant. These plants were grown on germination medium containing 0.8% (w/v) agar, half-strength Murashige-Skoog salts, 100 $\mu\text{g ml}^{-1}$ myo-inositol, 1 $\mu\text{g ml}^{-1}$ thiamine HCl, 0.5 $\mu\text{g ml}^{-1}$ pyridoxine, 0.5 $\mu\text{g ml}^{-1}$ nicotinic acid, 0.5 $\mu\text{g ml}^{-1}$ MES-KOH (pH 5.7), and 2% (w/v) sucrose. In some experiments, 2,4-dichlorophenoxybutyric acid (2,4-DB) was added, or sucrose was removed from the growth medium, as indicated. Germination was induced under continuous white light conditions at 22 °C, following incubation in the dark for 48 h at 4 °C. For treatment with proteasome inhibitors, 4-day-old dark-grown seedlings were vacuum-infiltrated for 10 min with liquid Murashige-Skoog medium containing 0.5% (v/v) dimethyl sulfoxide (DMSO) and 50 μM MG132 or 5 μM lactacystin and then incubated in the dark for 3 h. Control plants were treated with liquid Murashige-Skoog medium containing 0.5% (v/v) DMSO.

Immunoprecipitation—Immunoprecipitation was performed using μ MACS epitope tag protein isolation kits (Miltenyi Biotec). Whole seedlings of GFP-PEX7, GFP-PTS1, or GFP-PEX16 transgenic plants were grown under dark conditions for 5 days and homogenized with homogenization buffer (50 mM HEPES-NaOH, pH 8.0, 150 mM NaCl, and 0.25% (w/v) digitonin or 0.1% (w/v) *n*-dodecyl β -D-maltoside (DDM)) on ice. The homogenates were centrifuged at $100,000 \times g$ for 30 min at 4 °C. The collected supernatants were incubated for 30 min on ice with magnetic beads conjugated to an anti-GFP antibody (Miltenyi Biotec). The mixtures were then applied to μ Columns (Miltenyi Biotec), and beads were recovered in a magnetic field. The columns were washed three times with homogenization buffer, followed by elution of the protein complexes with the provided elution buffer (Miltenyi Biotec).

Peptide Preparation for Mass Spectrometry Analysis—In-gel digestion was performed to digest the isolated protein complex into peptides. The fractions eluted from the immunoprecipitations were subjected to SDS-PAGE. The gel was washed twice with distilled water (for LC/MS; Kanto Chemical Co. Inc.), three times with 30% (v/v) acetonitrile for 1 h, and once with 100% acetonitrile for 10 min and then dried in vacuum. The dried gel was incubated with reduction buffer (10 mM dithiothreitol and 25 mM ammonium bicarbonate) at 56 °C for 1 h and then in alkylation buffer (55 mM iodoacetamide and 25 mM ammonium bicarbonate) at 25 °C for 45 min and then washed twice with 25 mM ammonium bicarbonate. The samples were dehydrated by two 10-min incubations in dehydration buffer (50% (v/v) acetonitrile and 25 mM ammonium bicarbonate) and one 5-min incubation with 100% (v/v) acetonitrile and then digested with 0.1 mg/ml trypsin (Promega) in 25 mM ammonium bicarbonate at 37 °C for 16 h. The digested peptides were recovered with 5% (v/v) formic acid and 50% (v/v) acetonitrile and with 0.1% (v/v) acetic acid and 5% (v/v) acetonitrile, respectively. The extracted peptides were combined and filtered through a 0.45- μm filter (Millipore, Ultra free-MC 0.45- μm filter unit) by centrifugation at $15,000 \times g$ for 3 min to remove any debris. The samples were then subjected to mass spectrometric analysis using an LTQ-Orbitrap XL-HTC-PAL system (27).

Plasmid Construction—To generate the *GFP-RabE1c* and *GFP-RabA1e* constructs, cDNA fragments of each gene with *attB1* and *attB2* attached at their 5' and 3' ends, respectively, were amplified by RT-PCR using gene-specific primer sets (for *GFP-RabE1c*, 5'-AAAAAGCAGGCTCAATGGCTGCTCCACCTGCT-3' and 5'-AGAAAGCTGGGTTTAAAGTTCCACAGCATGCAG-3'; for *GFP-RabA1e*, 5'-AAAAAGCAGGCTTAATGGGAGCCTACAGAGCC-3' and 5'-AGAAAGCTGGTCTCAACCTGAGCAACAACCA-3') and cloned into the entry vector pDONR221 using the Gateway BP recombination method (Invitrogen). Subsequently, the vectors were transferred into the destination vector pUGW52 (kindly provided by Dr. Nakagawa, Shimane University) (28) using the Gateway LR recombination method (Invitrogen).

BiFC Assays—*RabE1c* and *PEX7* cDNAs were cloned into the pDONR221 vector and subsequently transferred into the destination vectors pGWCY and pNYGW (kindly provided by Dr. Nakagawa) (13, 29), respectively, to generate *RabE1c-cYFP* and *nYFP-PEX7*, using the BP and LR recombination methods as

RabE1c Regulates PEX7 Function

described above. The expression vector ptdGW (a gift from Dr. R. Y. Tsien, University of California), harboring the *tdTomato* gene, was used as a marker for transformation, and the vector ptdTomato-PTS1, harboring the *td-Tomato-PTS1* gene (13), was used as a marker for peroxisomes.

Standard procedures for transient expression experiments were described previously (13). Mixtures of the appropriate combinations of plasmids were coated on gold particles 1.0 μm in diameter and bombarded into leek epidermal cells using the PDS-1000/He biolistic particle delivery system (Bio-Rad), resulting in coexpression of these proteins in the same cells after a 20-h incubation in the dark at room temperature. Imaging analysis of transfected cells was performed using confocal laser scanning microscopy.

Confocal Laser Scanning Microscopy—The leek epidermis was observed using a Zeiss LSM 510 confocal laser scanning microscope. Lasers with wavelengths of 488, 514, and 543 nm were used for excitation of GFP, YFP, and RFP, respectively. For detection of emission, the following filters were used: 505–530 nm band pass for GFP, 520–555 nm band pass for YFP, and 560–615 nm band pass for RFP.

Immunoblot Analysis—Total proteins were extracted from each plant by homogenization in sample buffer (10 mM Tris-HCl, pH 6.5, 12% (v/v) glycerol, 5% (v/v) 2-mercaptoethanol, and 1% (w/v) SDS). Protein concentration was measured using the Bio-Rad protein assay, with bovine γ -albumin as the standard. Equal amounts of proteins as well as a standard molecular marker (prestained low range; Bio-Rad) were separated by SDS-PAGE and transferred to a Millipore GVHP (0.22- μm) membrane. Membranes were blocked in 5% (w/v) skim milk solubilized in TBS-Tween (50 mM Tris-HCl, 0.15 M NaCl, 0.05% (w/v) Tween 20, pH 7.5) for 1 h with shaking, immunolabeled with primary (1.5:10,000 (v/v)) and secondary (5:10,000 (v/v), ECL anti-rabbit IgG, GE Healthcare) antibodies, and visualized with Chemi-Lumi One reagent (Nacalai Tesque).

For subcellular fractionation, seedlings were homogenized in a high salt buffer (150 mM HEPES-KOH (pH 7.5), 500 mM NaCl), followed by centrifugation at 100,000 $\times g$ for 20 min to separate the soluble and membrane fractions. Equal amounts of protein from each fraction were subjected to immunoblot analysis.

RESULTS

Identification of GFP-PEX7-interacting Proteins by Proteomic Analysis—To further our understanding of the molecular mechanism that mediates PEX7 translocation, we conducted proteomic analysis to identify PEX7-binding proteins using transgenic *Arabidopsis* plants expressing GFP-tagged PEX7 (GFP-PEX7), PTS1 (GFP-PTS1), and PEX16 (GFP-PEX16) (12, 13, 25, 26). The fusion of GFP to PTS1 results in localization of GFP to the peroxisomal matrix. PEX16 is an integral peroxisomal membrane protein, and GFP-PEX16 was previously shown to localize to the peroxisomal membrane (30, 31). GFP-PTS1 and GFP-PEX16 plants were used as a reference in order to identify (and exclude) nonspecific contaminating proteins present in the GFP-PEX7 samples.

Seedlings of GFP-PEX7, GFP-PTS1, and GFP-PEX16 plants were homogenized in buffer containing DDM or digitonin and

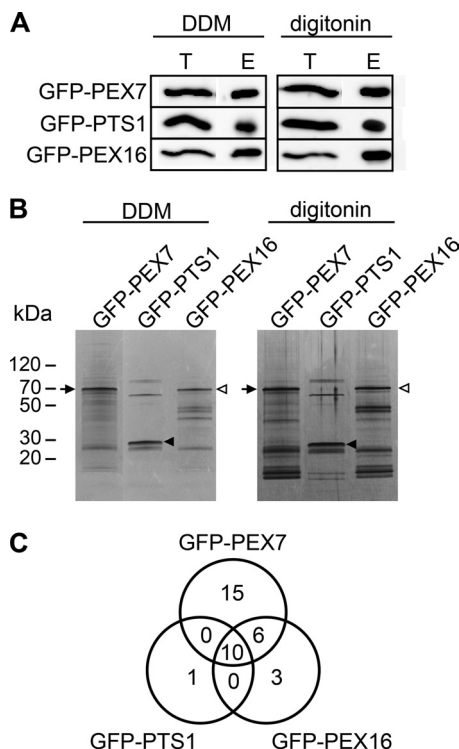


FIGURE 1. Isolation and identification of PEX-interacting proteins. A, isolation of GFP fusion proteins from transgenic *Arabidopsis* plants expressing GFP-PEX7, GFP-PTS1, and GFP-PEX16. Total extracts were prepared from the plants in the presence of either DDM or digitonin. The GFP fusion protein in the extracts was immunoprecipitated with an anti-GFP antibody. The amounts of fusion protein contained in 20 μl of total extract (T) or an equal volume of elution fraction (E) were compared by SDS-PAGE followed by immunoblot with an anti-GFP antibody. B, proteins that coimmunoprecipitated with the GFP fusion proteins. Proteins in the elution fraction were subjected to SDS-PAGE and visualized by silver staining. The transgenic plant type and the detergent used are indicated above each lane. The positions of the GFP-PEX7, GFP-PTS1, and GFP-PEX16 proteins are indicated by arrows, closed arrowheads, and open arrowheads, respectively. C, schematic representation of the number of proteins in affinity-purified fractions after MS/MS analysis. The Venn diagram represents the number of protein candidates that bind to each GFP fusion protein. Coimmunoprecipitated proteins in each elution fraction were identified by MS/MS analysis. Proteins detected in both DDM- and digitonin-treated fractions were identified as candidate binding proteins for the corresponding GFP-fusion protein.

incubated with anti-GFP antibody-conjugated microbeads prior to immunoprecipitation. GFP-PEX7 was efficiently affinity-purified, as determined by its presence in the purified fraction (Fig. 1A). In parallel, the purified fraction from each sample was subjected to separation by SDS-PAGE, followed by silver staining to visualize the proteins in purified fractions (Fig. 1B). In addition to GFP-PEX7 itself, whose molecular mass is about 60 kDa, a number of protein bands were detected in the GFP-PEX7 samples. Bands that were not present in the purified fractions from GFP-PTS1 or GFP-PEX16 plants were presumed to represent proteins that purified specifically with GFP-PEX7.

The eluted fractions were subjected to mass spectrometric analysis to identify the purified proteins. The results revealed that 230 proteins were co-immunoprecipitated with GFP-PEX7 in the presence of digitonin, and 418 proteins were co-immunoprecipitated in the presence of DDM. Then we presumed that the proteins that purified with GFP-PEX7 in both the digitonin and DDM experiments stably interact with PEX7, and we therefore selected these proteins as candidate PEX7-

TABLE 1**Proteins coimmunoprecipitated with GFP-PEX7 in the both DDM and digitonin experiments**

Arabidopsis Genome Initiative (AGI) codes and annotations were obtained from the TAIR database (available on the World Wide Web). Scores were calculated by Mascot (Matrix Science). Proteins with scores higher than 50 were selected.

AGI code	Annotation	DDM			Digitonin		
		Score	No. of identified peptides	Sequence coverage %	Score	No. of identified peptides	Sequence coverage %
AT1G29260.1	PEX7 (peroxin 7)	1764	11	34	1544	13	36
AT5G20890.1	T-complex protein 1, β subunit	573	14	21	278	11	14
AT3G20050.1	T-complex protein 1, α subunit	532	12	31	581	11	26
AT3G03960.1	T-complex protein 1, θ subunit	501	21	28	413	16	18
AT1G55490.1	CPN60B (chaperonin 60 β)	455	12	24	67	6	12
AT3G02530.1	T-complex protein 1, ζ subunit	420	14	20	243	11	17
AT5G16070.1	T-complex protein 1, ζ subunit	389	14	20	236	11	16
AT1G24510.1	T-complex protein 1, ϵ subunit	372	12	28	195	8	20
AT5G42080.1	DRP1A (dynamin-related protein 1A)	356	18	32	110	8	15
AT3G11830.1	T-complex protein 1, η subunit	318	10	13	288	9	13
AT3G18190.1	T-complex protein 1, δ subunit	296	13	32	209	11	21
AT5G26360.1	T-complex protein 1, γ subunit	190	12	17	200	11	14
AT5G56290.1	PEX5 (peroxin 5)	172	8	17	207	6	14
AT3G46060.1	AtRABE1c (<i>Arabidopsis</i> Rab GTPase homolog E1c)	78	6	33	55	4	21
AT4G18430.1	AtRABA1e (<i>Arabidopsis</i> Rab GTPase homolog A1e)	56	4	20	73	4	18

binding proteins. A total of 31 such proteins were identified, each with a protein score higher than 50 as calculated by the Mascot search engine. Of these proteins, 15 purified only with GFP-PEX7 and not with GFP-PTS1 or GFP-PEX16 (Fig. 1C and Table 1), indicating that those 15 proteins specifically bound to GFP-PEX7. Some of the proteins identified in this manner have been previously reported to bind to PEX7. For example, PEX5 is the PTS1 receptor and directly binds to PEX7 in plants (11, 13). We also identified eight subunits of the T-complex, which are homologs of the components of the mouse TCP1 complex (32), a cytosolic chaperonin. The T-complex binds to the WD40 repeat of PEX7 in yeast and animal cells (33, 34).

RabE1c Interacts with PEX7 and Partially Localizes to Peroxisomes—Two small GTPases, RabE1c and RabA1e, were newly identified in our experiment (Table 1). We examined the subcellular localization of RabE1c and RabA1e by transiently expressing GFP-RabE1c and GFP-RabA1e in leek epidermal cells (Fig. 2). GFP-RabE1c was observed predominantly in the cytosol, peroxisomes, and unidentified particles (Fig. 2A). The punctate structures distinct from the peroxisomes might represent the Golgi complex, because RabE1d, another member of the RabE1 family, is localized to the Golgi complex and cytosol in *Arabidopsis* (35). GFP-RabA1e was localized in the cytosol and to particulate structures distinct from peroxisomes (Fig. 2B). These results suggest that RabE1c interacts with PEX7 on the peroxisome.

To confirm the interaction between PEX7 and RabE1c *in vivo*, we performed a BiFC assay. To this end, we constructed two chimeric genes, one encoding the N-terminal half of YFP fused to PEX7 (nYFP-PEX7) and the other encoding the C-terminal half of YFP fused to RabE1c (RabE1c-cYFP). These pro-

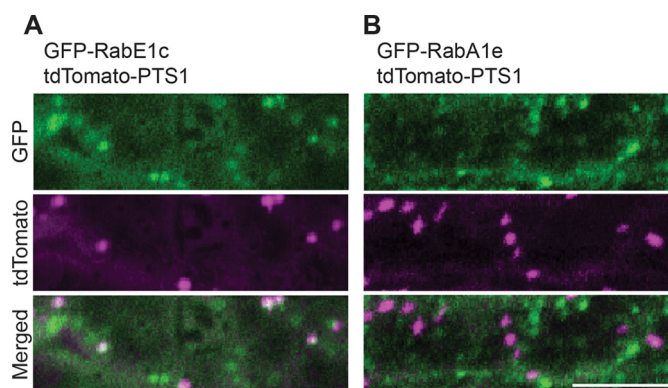


FIGURE 2. Subcellular localization of RabE1c and RabA1e. Either GFP-RabE1c (A) or GFP-RabA1e (B) was introduced, along with tdTomato-PTS1, into leek epidermal cells. GFP and tdTomato fluorescence in the cells was visualized by confocal laser scanning microscopy. The green color shown in the top and bottom panels represents fluorescence derived from the GFP fusion proteins, whereas the magenta color in the middle and bottom panels represents fluorescence derived from tdTomato-PTS1. White spots in the merged image (A, bottom) indicate peroxisomes containing both GFP-RabE1c and tdTomato-PTS1. Scale bar, 10 μ m.

teins, along with tdTomato-PTS1, a peroxisomal marker, were transiently expressed in leek epidermal cells. As shown in Fig. 3A, YFP fluorescence was observed exclusively on peroxisomes, as identified by the red fluorescent signal of tdTomato-PTS1. No signal was detected in control cells expressing RabE1c-cYFP and nYFP (Fig. 3B) or cYFP and nYFP-PEX7 (Fig. 3C). These results indicate that PEX7 and RabE1c specifically interact with each other on peroxisomes *in vivo*.

The Active Form of RabE1c Interacts with PEX7—To determine whether GTP binding is crucial for the interaction of RabE1c with PEX7, we generated three mutant forms of RabE1c

RabE1c Regulates PEX7 Function

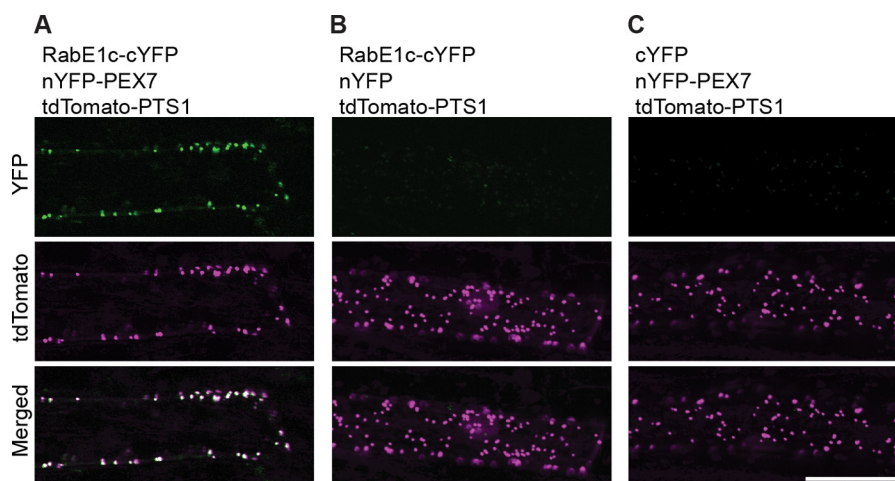


FIGURE 3. **BiFC analysis of the interaction between RabE1c and PEX7.** *A*, top, RabE1c-cYFP and nYFP-PEX7 were co-expressed in leek epidermal cells. Fluorescence derived from reconstituted YFP was visualized by confocal laser scanning microscopy. As negative controls, fluorescence was also examined in cells co-expressing RabE1c-cYFP/nYFP (*B*, top) and cYFP/nYFP-PEX7 (*C*, top). In all cases, tdTomato-PTS1 was simultaneously expressed as a marker for peroxisomes (*A–C*, middle and bottom). White spots in the merged image (*A*, bottom) indicate colocalization of YFP and tdTomato fluorescence. Scale bar, 50 μ m.

containing amino acid substitutions: Ser-29 to Asn (RabE1c(S29N)), Gln-74 to Leu (RabE1c(Q74L)), and Asn-128 to Ile (RabE1c(N128I)). In many Rab- and Ras-like GTPases, these amino acid substitutions correspond to RabE1c mutations that alter nucleotide affinity, resulting in either a GDP-bound dominant negative form or a GTP-bound constitutively active form (36). RabE1c(S29N) and RabE1c(N128I) are predicted to be the GDP-bound dominant negative forms, and RabE1c(Q74L) should produce the GTP-bound constitutively active form. Each construct was fused to cYFP and expressed in leek epidermal cells along with nYFP-PEX7. A punctate fluorescent signal was observed only in cells co-expressing RabE1c(Q74L)-cYFP and nYFP-PEX7 (Fig. 4C). The observed green punctate structures were the same as the structures identified as peroxisomes in cells expressing wild-type RabE1c-cYFP and nYFP-PEX7 (Fig. 3A). No signal was detected in cells expressing either RabE1c(S29N)-cYFP and nYFP-PEX7 (Fig. 4B) or RabE1c(N128I)-cYFP and nYFP-PEX7 (Fig. 4D). These results indicate that GTP-bound RabE1c, but not GDP-bound RabE1c, interacts with PEX7.

GFP-PEX7 Expression Reduces Peroxisomal β -Oxidation, and RabE1c Deficiency Restores the Effects of GFP-PEX7 in *Arabidopsis*—PEX7 is involved in various functions related to peroxisomal protein transport. Therefore, we assessed the involvement of the PEX7-binding protein RabE1c in peroxisome function. To analyze the physiological role of RabE1c, we used an *Arabidopsis rabe1c* knock-out mutant. Peroxisomal fatty acid β -oxidation is the main pathway for the catabolism of seed-reserved lipids. This pathway also converts 2,4-DB to 2,4-D, which inhibits root elongation at an early stage of seedling growth in *Arabidopsis* (37). Therefore, mutants with deficient peroxisomal β -oxidation are resistant to 2,4-DB but sensitive to 2,4-D (37). 2,4-DB sensitivity was evaluated by monitoring the seedling growth of *rabe1c* knock-out plants. The root growth of *rabe1c* seedlings during germination was sensitive to 2,4-DB to an extent similar to that of wild-type plants (Fig. 5). Peroxisomal fatty acid β -oxidation is responsible for the mobilization of seed-reserved lipid into sucrose in seed-

lings. Therefore, mutants with deficient peroxisomal β -oxidation require exogenously applied sucrose for successful establishment of seedlings (37, 38). The *rabe1c* seedlings grew without sucrose as well as wild-type seedlings did (Fig. 5). These findings indicate that peroxisomal fatty acid β -oxidation is not impaired in the *rabe1c* mutant seedlings. Next, we examined the growth of GFP-PEX7-expressing plants (Fig. 1). In addition, we crossed *rabe1c* with GFP-PEX7 plants to generate GFP-PEX7/*rabe1c* plants, and the growth of these plants was examined under the same conditions. The GFP-PEX7 seedlings were resistant to 2,4-DB and required exogenous sucrose for germination (Fig. 5, *A* and *B*), indicating that the expression of GFP-PEX7 results in reduced peroxisomal β -oxidation activity. This finding suggests that GFP-PEX7 has a negative effect on peroxisome biogenesis. However, this phenotype was rescued by the *rabe1c* mutation in GFP-PEX7 plants, as demonstrated by the observation that GFP-PEX7/*rabe1c* seedlings were 2,4-DB-sensitive and sucrose-independent to a degree similar to wild-type plants (Fig. 5, *A* and *B*). This result shows that defective peroxisomal β -oxidation in GFP-PEX7 seedlings can be restored by the loss of RabE1c function.

GFP-PEX7 Expression Reduces Peroxisomal Protein Transport, and RabE1c Deficiency Restores Peroxisomal Protein Transport in GFP-PEX7-expressing Plants—Because defective peroxisomal β -oxidation is often attributed to reduced transport of peroxisomal matrix enzymes, we measured the peroxisomal import of 3-ketoacyl-CoA thiolase, a PTS2-containing protein that catalyzes the last step of β -oxidation. *Arabidopsis* PTS2-containing proteins are synthesized in the cytosol as longer precursor peptides. After entry into peroxisomes, they are processed into their mature forms via the removal of their PTS2 sequences by the peroxisomal protease DEG15 endopeptidase (6). Accumulation of the 3-ketoacyl-CoA thiolase precursor was detected in *pex7i* knockdown plants, as previously reported (Fig. 6) (12). This thiolase precursor was not detected in the *rabe1c* mutant seedlings (Fig. 6), indicating that the import of PTS2-containing proteins occurs normally in the absence of RabE1c. By contrast, a significant amount of thiolase precursor

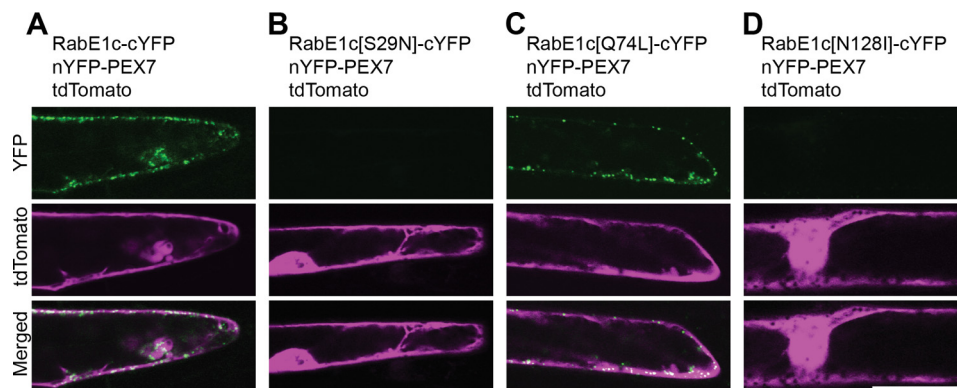


FIGURE 4. **The constitutively active form but not the dominant negative form of RabE1c interacts with PEX7.** Confocal microscopic images of leek epidermal cells were acquired after coexpression of nYFP-PEX7 with RabE1c-cYFP (A), RabE1c(S29N)-cYFP (B), RabE1c(Q74L)-cYFP (C), and RabE1c(N128I)-cYFP (D). YFP fluorescence (A and C, top panels) represents reconstituted YFP molecules. Cytosolic tdTomato was simultaneously expressed in all experiments as a marker of transformed cells. Scale bar, 50 μ m.

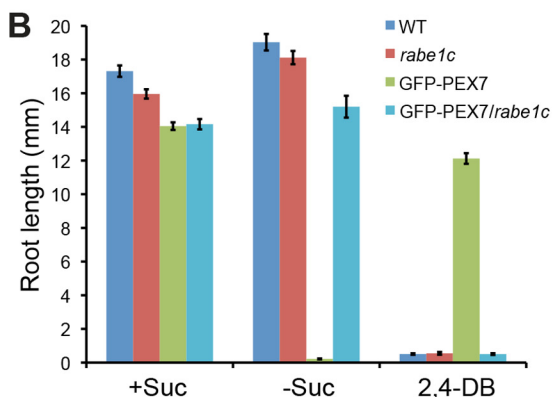
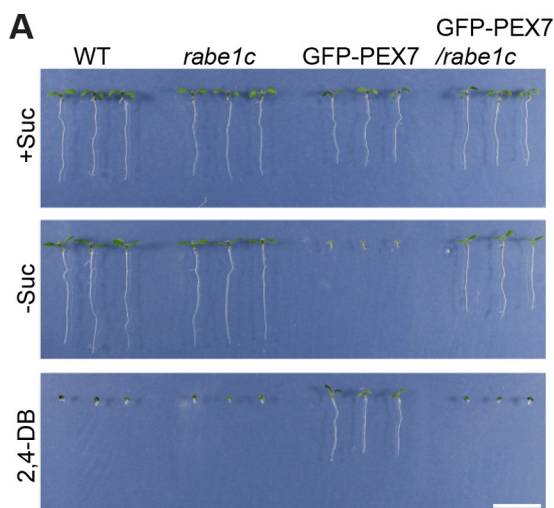


FIGURE 5. **The effect of sucrose and 2,4-DB on the growth of *rabe1c* mutant plants.** A, wild-type plants, *rabe1c* mutant (*rabe1c*) transgenic plants expressing GFP-PEX7 (GFP-PEX7), and *rabe1c* mutant transgenic plants expressing GFP-PEX7 (GFP-PEX7/*rabe1c*) were grown in the presence (+Suc) or absence (–Suc) of sucrose for 6 days under continuous illumination. These plants were also grown in the presence of 0.5 μ g/ml 2,4-DB. Scale bar, 1 cm. B, root lengths of the seedlings shown in A. Data represent the means \pm S.D. (error bars) ($n = 12$) in mm.

was detected in the GFP-PEX7 seedlings (Fig. 6), suggesting that the import of PTS2-containing proteins is reduced in these plants. These results were consistent with the defect in peroxisomal β -oxidation observed in the GFP-PEX7 plants (Fig. 5). By contrast, almost no thiolase precursor was detected in the GFP-

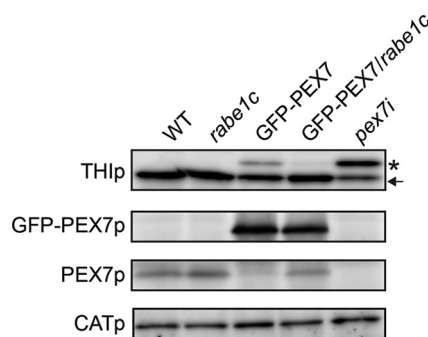


FIGURE 6. **Transport of PTS2-containing proteins and endogenous levels of PEX7 in mutant seedlings.** Equal amounts of homogenate (50 μ g for GFP-PEX7p and PEX7p, 10 μ g for CATp) from dark-grown wild-type, *rabe1c*, GFP-PEX7, GFP-PEX7/*rabe1c*, and *pex7i* seedlings were separated by SDS-PAGE followed by immunoblot analysis to detect 3-ketoacyl-CoA thiolase (TH1p), GFP-PEX7 (GFP-PEX7p), endogenous PEX7 (PEX7p), and catalase (CATp). The protein level of catalase, which was used as a loading control, was the same in each sample. An asterisk and an arrow indicate the precursor and mature forms of thiolase, respectively.

PEX7/*rabe1c* seedlings (Fig. 6), indicating that the *rabe1c* mutation diminished the effect of GFP-PEX7 expression. This result was consistent with the rescue of peroxisomal β -oxidation in GFP-PEX7/*rabe1c* plants observed during germination (Fig. 5).

Degradation of Endogenous Soluble PEX7 Is Dependent on RabE1c in GFP-PEX7-expressing Plants—Because PEX7 is responsible for the import of PTS2 proteins, we measured the expression levels of PEX7 protein in wild-type and mutant plants (Fig. 6). The amount of endogenous PEX7 was the same in *rabe1c* and wild-type plants, but the level was reduced in GFP-PEX7 seedlings. This result indicates that expression of GFP-PEX7 protein reduces the level of endogenous PEX7, leading to reduced import of PTS2-containing proteins. However, endogenous PEX7 protein was restored to wild-type levels in the GFP-PEX7/*rabe1c* transgenic plants, indicating that RabE1c is involved in GFP-PEX7-induced reduction of PEX7. No significant difference in the level of GFP-PEX7 protein was observed between GFP-PEX7 and GFP-PEX7/*rabe1c* plants.

In *Arabidopsis*, PEX7 is mainly localized to the cytosol (13). To determine whether the reduction in PEX7 accumulation in GFP-PEX7 plants occurs in the cytosol, homogenates prepared from 5-day-old dark-grown seedlings were separated into sol-

RabE1c Regulates PEX7 Function

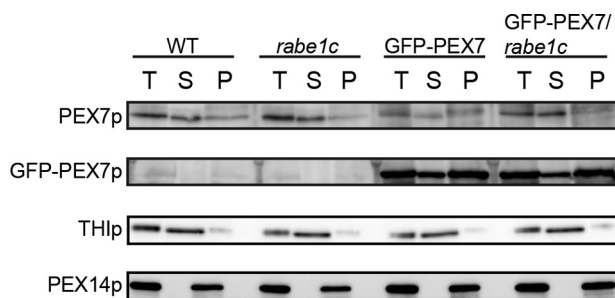


FIGURE 7. Endogenous cytosolic PEX7 is degraded in GFP-PEX7 seedlings and restored in GFP-PEX7/*rabe1c* seedlings. Five-day-old dark-grown wild-type, *rabe1c*, GFP-PEX7, and GFP-PEX7/*rabe1c* seedlings were homogenized in high salt buffer containing 500 mM NaCl. Total extract (T) was centrifuged at $100,000 \times g$ to separate the supernatant (S) and membrane (P) fractions. Equal amounts of homogenate (50 μ g for GFP-PEX7 and endogenous PEX7, 10 μ g for 3-ketoacyl-CoA thiolase and PEX14) were separated by SDS-PAGE, followed by immunoblot analysis to detect 3-ketoacyl-CoA thiolase (TH1p), GFP-PEX7 (GFP-PEX7p), endogenous PEX7 (PEX7p), and PEX14p. Thiolase and PEX14 were used as markers of peroxisomal matrix and membrane proteins, respectively.

uble and membrane fractions by centrifugation at $100,000 \times g$. These fractions were then separated by SDS-PAGE and subjected to immunoblot analysis (Fig. 7). Two peroxisomal proteins, thiolase and PEX14, were used as markers of soluble and membrane fractions, respectively (17, 37). As expected, thiolase and PEX14 were recovered in the soluble and membrane fractions, respectively, confirming that the fractionation technique was effective (Fig. 7). In wild-type plants, the majority of PEX7 was recovered in the soluble fraction (Fig. 7). The *rabe1c* mutant exhibited a similar PEX7 level and accumulation pattern to that of wild-type plants (Fig. 7). In the GFP-PEX7 plants, however, the PEX7 level was significantly reduced in the soluble fraction, whereas its level in the membrane fraction remained similar to that of wild-type plants, indicating a reduction in cytosolic PEX7. The level of soluble PEX7 was restored to that of wild-type plants in the GFP-PEX7/*rabe1c* transgenic plant, indicating that loss of RabE1c activity increased the cytosolic proportion of PEX7 in the GFP-PEX7 plants.

Surprisingly, in contrast to endogenous PEX7, the GFP-PEX7 fusion protein was abundant in the insoluble membrane fraction in both the GFP-PEX7 and GFP-PEX7/*rabe1c* seedlings (Fig. 7). GFP-PEX7 protein levels were identical in these two types of seedlings in both the soluble and membrane fractions. These findings suggest that, unlike PEX7, GFP-PEX7 is stacked on the peroxisomal membrane and is not dislocated to the cytosol by its defective release from the peroxisomal membrane in GFP-PEX7 and GFP-PEX7/*rabe1c* plants.

The Proteasome Is Responsible for the Degradation of Endogenous PEX7 in GFP-PEX7-expressing Plants—PEX7 is targeted to peroxisomes and then dislocated into the cytosol in yeast and mammals (39, 40). In yeast, membrane binding of PEX7 requires the auxiliary proteins PEX18 and PEX20 (14, 41). These auxiliary proteins are polyubiquitinated at the last step of dislocation, a modification that destines them for degradation via the 26 S proteasome (15, 41). However, it is not known whether PEX7 is degraded by the proteasome. To determine whether the reduction of PEX7 expression involves proteasome-mediated degradation in the GFP-PEX7 plants, we examined the effect of two proteasome inhibitors, MG132 and lacta-

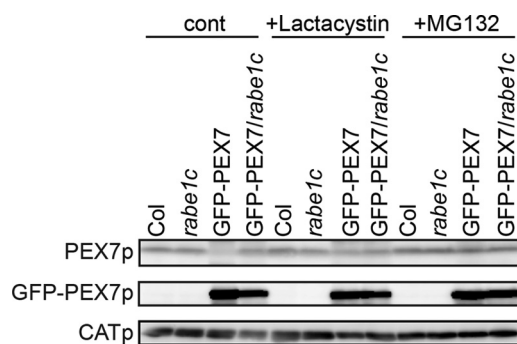


FIGURE 8. Effect of 26 S proteasome inhibitors on the levels of endogenous PEX7. Four-day-old dark-grown wild-type, *rabe1c*, GFP-PEX7, and GFP-PEX7/*rabe1c* seedlings were transferred to liquid Murashige-Skoog medium containing 50 μ M MG132 or 5 μ M lactacystin and incubated for 3 h in the dark. Proteins were then extracted from whole seedlings. Equal amounts of total protein (50 μ g) were separated by SDS-PAGE followed by immunoblot analyses to detect PEX7 and GFP-PEX7. Catalase (CATp) was used as a loading control.

cystin. Seedlings were treated with either inhibitor for 3 h and homogenized, and PEX7 protein levels were determined by immunoblot analysis. As shown in Fig. 8, the PEX7 protein level was significantly increased in GFP-PEX7 plants after proteasome inhibitor treatment, to a level comparable with that in GFP-PEX7/*rabe1c* plants. Neither inhibitor had any effect on the level of PEX7 in wild-type or *rabe1c* mutant plants, indicating that PEX7 is degraded by the proteasome in the presence of GFP-PEX7.

DISCUSSION

Identification of PEX7-binding Proteins by Proteomic Analysis—Previously, we showed that PEX7 can bind PEX5 in *Arabidopsis* (11, 13). PEX7 contains a WD40 repeat, a sequence known to bind the T-complex, a cytosolic chaperonin (33, 34). During the course of this study, we identified PEX5 and all subunits of the T-complex as GFP-PEX7-associated proteins (Table 1). The *Arabidopsis* genome contains nine genes encoding the T-complex subunits α , β , γ , δ , ϵ , ζ 1, ζ 2, η , and θ , which are similar to those of the mouse T-complex, TCP-1. It should be noted that all of these subunits were identified in this study, suggesting that the T-complex may bind PEX7 in the cytosol of *Arabidopsis*. In addition to these known PEX7-binding proteins, we identified five new proteins as novel candidates for PEX7-binding proteins, including two small GTPases. Based on increasing evidence for the relationship between small GTPases and peroxisomes (42, 43), we further investigated the involvement of these proteins in peroxisomal biogenesis. Although *Arabidopsis* Rab GTPases share highly similar amino acid sequences, proteomic analysis identified only RabE1c and RabA1e as potential PEX7-binding proteins. The peroxisomal localization of RabE1c suggested that RabE1c interacts with PEX7 on the peroxisomal membrane. Consistent with this, we demonstrated that the *in vivo* interaction between PEX7 and RabE1c occurs on peroxisomes (Fig. 3). GTP-bound active RabE1c, but not GDP-bound inactive RabE1c, can bind specifically to PEX7 (Fig. 4), suggesting that RabE1c regulates PEX7 expression levels by binding to and dissociating from PEX7 during the GDP/GTP cycle.

RabE-type GTPase Is a Regulatory Factor of Peroxisomes—Rab GTPases are widely distributed across eukaryotic organisms and comprise eight subfamilies in *Arabidopsis* (44). These Rab GTPases are involved primarily in membrane traffic, and most are localized to components of the secretory pathway (45). However, some GTPases are involved not only in membrane traffic but also in other cellular mechanisms. In mammals, RhoA, Rho kinase II, and Rab8a, a close homolog of *Arabidopsis* RabE1c, are associated with peroxisomes and cooperate in peroxisome-cytoskeleton interactions (43). When we examined the subcellular localization of GFP-tagged AtRabE1c, we found that it partially localized to peroxisomes, suggesting that RabE1c is also involved in peroxisomal biogenesis in plants.

GFP-PEX7 Expression Decreases Peroxisomal Protein Transport as a Result of a Reduction in the Endogenous PEX7 Level—After cargo release, PEX7 in yeast and mammalian cells is dislocated into the cytosol for the next round of import (39, 40). Therefore, PEX7 is localized predominantly in the cytosol in wild-type cells. We found, however, that the GFP-PEX7 fusion protein behaves significantly differently from endogenous PEX7. Cell fractionation analysis revealed that PEX7 is present mainly in the soluble fraction, which presumably represents the cytosol, whereas GFP-PEX7 was mainly observed in the insoluble membrane fraction (Fig. 7). These data suggest that release of GFP-PEX7 from the peroxisome is impaired, resulting in its accumulation in the membrane fraction. Similar phenomena have been reported in *S. cerevisiae* and mammalian cells, in which PEX7 tagged with either HA or GFP localizes to the peroxisome membrane (46, 47), suggesting that tagged PEX7 cannot be dislocated from the peroxisome. We also found that expression of GFP-PEX7 has a dominant negative effect on peroxisomal function; a defect in peroxisomal β -oxidation was observed in the GFP-PEX7-expressing plants (Fig. 5), as was a defect in PTS2 protein import (Fig. 6). This defect was accompanied by a reduction in the level of endogenous PEX7 (Fig. 6) relative to the level in wild-type plants.

The mechanism by which GFP-PEX7 causes the degradation of endogenous PEX7 remains unclear. One potential explanation may be that the decrease in PEX7 accumulation is mediated by the quality control system (23). This system is illustrated by the fate of PEX5, a PTS1 receptor, in specific mutant backgrounds. In wild-type cells, PEX5 is normally dislocated into the cytosol upon monoubiquitination. However, in mutants defective in receptor dislocation, such as *P. pastoris* *pex1*, *pex4*, *pex6*, and *pex22*, human *pex1* and *pex6*, and *Arabidopsis* *pex6*, PEX5 accumulates in the peroxisome and becomes polyubiquitinated and targeted for subsequent degradation by the 26 S proteasome (18, 22, 48, 49). In these mutants, PEX5 levels are depleted, thereby impairing the import of peroxisomal proteins. This type of quality control may also operate for PEX7 degradation. We propose that high levels of membrane-stacked GFP-PEX7 stress the peroxisomal membrane, or GFP-PEX7 and PEX7 may dimerize with each other, leading both proteins to be recognized as targets for degradation. However, the observation that the level of GFP-PEX7 does not change suggests that GFP-PEX7 is resistant to degradation. It is possible that the GFP domain of GFP-PEX7 blocks the ubiquitination site in PEX7, which is responsible for both dislocation and

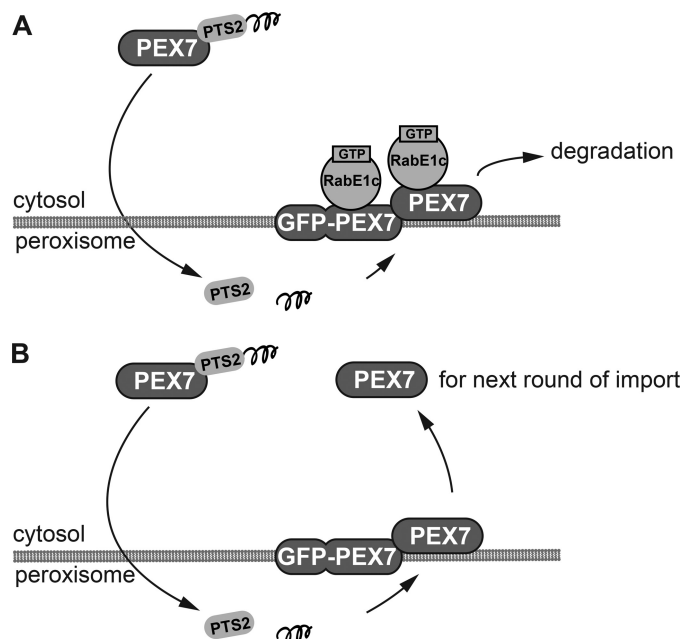


FIGURE 9. Model for the role of RabE1c during dislocation of PEX7 from the peroxisomal membrane. *A*, in GFP-PEX7 plants, after the PEX7 receptor-cargo (PTS2-containing protein) complex is imported into the peroxisomes, PEX7 is stacked on the peroxisomal membrane together with GFP-PEX7. The GTP-bound form of RabE1c on the peroxisomal membrane then recruits stacked PEX7 to the 26 S proteasome for degradation. RabE1c also binds to GFP-PEX7 but cannot recruit it to the 26 S proteasome for degradation. *B*, in GFP-PEX7/*rabe1c* plants, the degradation of PEX7 is inhibited, and PEX7 is dislocated into the cytosol for the next round of cargo import. GFP-PEX7 cannot be released into the cytosol and remains on the peroxisomal membrane.

proteasome-dependent degradation. Consistent with this, fusion of GFP to the C terminus of PEX7 impairs its dislocation in yeast and mammalian cells (40, 47). In addition, another group has presented evidence that the fusion of a Myc tag to the N terminus of PEX5 interferes with polyubiquitination and subsequent degradation (24). These results suggest that fused polypeptide tags interfere with the removal of transport receptors from the peroxisomal membrane.

PEX7 Degradation Depends on RabE1c—The simple *rabe1c* knock-out mutant did not exhibit any peroxisomal defects, suggesting that *RabE1c* is dispensable for peroxisome function in the wild-type background, at least under our experimental conditions. However, we found that mutation of *rabe1c* reversed the defects in peroxisomal function and peroxisomal protein transport in the GFP-PEX7 background, suggesting that RabE1c is involved in the maintenance of PEX7 quality when abnormal PEX7 accumulates on the peroxisome membrane. A model outlining this mechanism is shown in Fig. 9.

In GFP-PEX7 seedlings (Fig. 9A), endogenous PEX7 is degraded via the 26 S proteasome. In GFP-PEX7/*rabe1c* mutants (Fig. 9B), although the same amount of GFP-PEX7 protein accumulates on the peroxisomal membranes as in GFP-PEX7 plants, endogenous PEX7 is restored almost to the level in wild-type plants (Fig. 6). Therefore, RabE1c is responsible for the degradation of endogenous PEX7 in the presence of GFP-PEX7. The protein level of soluble PEX7 was restored in the GFP-PEX7/*rabe1c* mutant seedlings (Fig. 7), suggesting that RabE1c dysfunction increases cytosolic PEX7 in the GFP-PEX7

RabE1c Regulates PEX7 Function

background. In addition, PTS2-containing protein import (Fig. 6) and peroxisomal β -oxidation (Fig. 5) were restored. Thus, endogenous cytosolic PEX7, rather than membrane-bound GFP-PEX7, is essential for transport of PTS2-containing proteins.

A recent study showed that the degradation of the import machinery residing on the outer membrane of plastids occurs in the plastid outer membrane and is regulated by a ubiquitin E3 ligase (50). In our study, we identified RabE1c as a novel PEX7-binding protein involved in targeting PEX7 for degradation when abnormal PEX7 is present on the peroxisomal membrane. Our findings also demonstrate that our proteomic analysis can specifically and effectively identify new regulatory components and highlight the potential utility of performing similar experiments to examine the regulation of other PEXs.

Acknowledgments—We thank Dr. Tsuyoshi Nakagawa (Shimane University) for providing the pUGW, pGWcY, and pnYGW vectors; Dr. Roger Y. Tsien (University of California, San Diego) for providing the tdTomato vector; and the staff of the core research facilities and model plant resource facilities at the National Institute for Basic Biology for plant maintenance and technical support.

REFERENCES

- Hayashi, M., Aoki, M., Kato, A., Kondo, M., and Nishimura, M. (1996) Transport of chimeric proteins that contain a carboxyl-terminal targeting signal into plant microbodies. *Plant J.* **10**, 225–234
- Kato, A., Hayashi, M., Takeuchi, Y., and Nishimura, M. (1996) cDNA cloning and expression of a gene for 3-ketoacyl-CoA thiolase in pumpkin cotyledons. *Plant Mol. Biol.* **31**, 843–852
- Kato, A., Hayashi, M., Kondo, M., and Nishimura, M. (1996) Targeting and processing of a chimeric protein with the N-terminal presequence of the precursor to glyoxysomal citrate synthase. *Plant Cell* **8**, 1601–1611
- Kato, A., Takeda-Yoshikawa, Y., Hayashi, M., Kondo, M., Hara-Nishimura, I., and Nishimura, M. (1998) Glyoxysomal malate dehydrogenase in pumpkin. Cloning of a cDNA and functional analysis of its presequence. *Plant Cell Physiol.* **39**, 186–195
- Hayashi, H., De Bellis, L., Yamaguchi, K., Kato, A., Hayashi, M., and Nishimura, M. (1998) Molecular characterization of a glyoxysomal long chain acyl-CoA oxidase that is synthesized as a precursor of higher molecular mass in pumpkin. *J. Biol. Chem.* **273**, 8301–8307
- Schuhmann, H., Huesgen, P. F., Gietl, C., and Adamska, I. (2008) The DEG15 serine protease cleaves peroxisomal targeting signal 2-containing proteins in *Arabidopsis*. *Plant Physiol.* **148**, 1847–1856
- Kragler, F., Lametschwandtner, G., Christmann, J., Hartig, A., and Harada, J. J. (1998) Identification and analysis of the plant peroxisomal targeting signal 1 receptor NtPEX5. *Proc. Natl. Acad. Sci. U.S.A.* **95**, 13336–13341
- Woodward, A. W., and Bartel, B. (2005) The *Arabidopsis* peroxisomal targeting signal 2 receptor PEX7 is necessary for peroxisome function and dependent on PEX5. *Mol. Cell Biol.* **25**, 573–583
- Matsumura, T., Otera, H., and Fujiki, Y. (2000) Disruption of the interaction of the longer isoform of Pex5p, Pex5pL, with Pex7p abolishes peroxisome targeting signal type 2 protein import in mammals. Study with a novel Pex5-impaired Chinese hamster ovary cell mutant. *J. Biol. Chem.* **275**, 21715–21721
- Otera, H., Harano, T., Honsho, M., Ghaedi, K., Mukai, S., Tanaka, A., Kawai, A., Shimizu, N., and Fujiki, Y. (2000) The mammalian peroxin Pex5pL, the longer isoform of the mobile peroxisome targeting signal (PTS) type 1 transporter, translocates the Pex7p.PTS2 protein complex into peroxisomes via its initial docking site, Pex14p. *J. Biol. Chem.* **275**, 21703–21714
- Nito, K., Hayashi, M., and Nishimura, M. (2002) Direct interaction and determination of binding domains among peroxisomal import factors in *Arabidopsis thaliana*. *Plant Cell Physiol.* **43**, 355–366
- Hayashi, M., Yagi, M., Nito, K., Kamada, T., and Nishimura, M. (2005) Differential contribution of two peroxisomal protein receptors to the maintenance of peroxisomal functions in *Arabidopsis*. *J. Biol. Chem.* **280**, 14829–14835
- Singh, T., Hayashi, M., Mano, S., Arai, Y., Goto, S., and Nishimura, M. (2009) Molecular components required for the targeting of PEX7 to peroxisomes in *Arabidopsis thaliana*. *Plant J.* **60**, 488–498
- Einwächter, H., Sowinski, S., Kunau, W. H., and Schliebs, W. (2001) Yarrowia lipolytica Pex20p, *Saccharomyces cerevisiae* Pex18p/Pex21p and mammalian Pex5pL fulfill a common function in the early steps of the peroxisomal PTS2 import pathway. *EMBO Rep.* **2**, 1035–1039
- Léon, S., Zhang, L., McDonald, W. H., Yates, J., 3rd, Cregg, J. M., and Subramani, S. (2006) Dynamics of the peroxisomal import cycle of PpPex20p. Ubiquitin-dependent localization and regulation. *J. Cell Biol.* **172**, 67–78
- Sichting, M., Schell-Steven, A., Prokisch, H., Erdmann, R., and Rottensteiner, H. (2003) Pex7p and Pex20p of *Neurospora crassa* function together in PTS2-dependent protein import into peroxisomes. *Mol. Biol. Cell* **14**, 810–821
- Hayashi, M., Nito, K., Toriyama-Kato, K., Kondo, M., Yamaya, T., and Nishimura, M. (2000) AtPex14p maintains peroxisomal functions by determining protein targeting to three kinds of plant peroxisomes. *EMBO J.* **19**, 5701–5710
- Koller, A., Snyder, W. B., Faber, K. N., Wenzel, T. J., Rangell, L., Keller, G. A., and Subramani, S. (1999) Pex22p of *Pichia pastoris*, essential for peroxisomal matrix protein import, anchors the ubiquitin-conjugating enzyme, Pex4p, on the peroxisomal membrane. *J. Cell Biol.* **146**, 99–112
- Zolman, B. K., Monroe-Augustus, M., Silva, I. D., and Bartel, B. (2005) Identification and functional characterization of *Arabidopsis* PEROXIN4 and the interacting protein PEROXIN22. *Plant Cell* **17**, 3422–3435
- Okumoto, K. (2000) Molecular anatomy of the peroxin Pex12p. Ring finger domain is essential for Pex12p function and interacts with the peroxisome-targeting signal type 1-receptor Pex5p and a ring peroxin, Pex10p. *J. Biol. Chem.* **275**, 25700–25710
- Platta, H. W., El Magraoui, F., Bäumer, B. E., Schlee, D., Girzalsky, W., and Erdmann, R. (2009) Pex2 and Pex12 function as protein-ubiquitin ligases in peroxisomal protein import. *Mol. Cell Biol.* **29**, 5505–5516
- Zolman, B. K., and Bartel, B. (2004) An *Arabidopsis* indole-3-butyric acid-response mutant defective in PEROXIN6, an apparent ATPase implicated in peroxisomal function. *Proc. Natl. Acad. Sci. U.S.A.* **101**, 1786–1791
- Kiel, J. A., Emmrich, K., Meyer, H. E., and Kunau, W. H. (2005) Ubiquitination of the peroxisomal targeting signal type 1 receptor, Pex5p, suggests the presence of a quality control mechanism during peroxisomal matrix protein import. *J. Biol. Chem.* **280**, 1921–1930
- Platta, H. W., El Magraoui, F., Schlee, D., Grunau, S., Girzalsky, W., and Erdmann, R. (2007) Ubiquitination of the peroxisomal import receptor Pex5p is required for its recycling. *J. Cell Biol.* **177**, 197–204
- Mano, S., Nakamori, C., Hayashi, M., Kato, A., Kondo, M., and Nishimura, M. (2002) Distribution and characterization of peroxisomes in *Arabidopsis* by visualization with GFP. Dynamic morphology and actin-dependent movement. *Plant Cell Physiol.* **43**, 331–341
- Nito, K., Kamigaki, A., Kondo, M., Hayashi, M., and Nishimura, M. (2007) Functional classification of *Arabidopsis* peroxisome biogenesis factors proposed from analyses of knockdown mutants. *Plant Cell Physiol.* **48**, 763–774
- Tamura, K., Fukao, Y., Iwamoto, M., Haraguchi, T., and Hara-Nishimura, I. (2010) Identification and characterization of nuclear pore complex components in *Arabidopsis thaliana*. *Plant Cell* **22**, 4084–4097
- Nakagawa, T., Suzuki, T., Murata, S., Nakamura, S., Hino, T., Maeo, K., Tabata, R., Kawai, T., Tanaka, K., Niwa, Y., Watanabe, Y., Nakamura, K., Kimura, T., and Ishiguro, S. (2007) Improved Gateway binary vectors. High-performance vectors for creation of fusion constructs in transgenic analysis of plants. *Biosci. Biotechnol. Biochem.* **71**, 2095–2100
- Hino, T., Tanaka, Y., Kawamukai, M., Nishimura, K., Mano, S., and Nakagawa, T. (2011) Two Sec13p homologs, AtSec13A and AtSec13B, redundantly contribute to formation of COPII transport vesicles in *Arabidopsis thaliana*. *Biosci. Biotechnol. Biochem.* **75**, 1848–1852

30. Karnik, S. K., and Trelease, R. N. (2005) *Arabidopsis* peroxin 16 coexists at steady state in peroxisomes and endoplasmic reticulum. *Plant Physiol.* **138**, 1967–1981
31. Lin, Y., Cluette-Brown, J. E., and Goodman, H. M. (2004) The peroxisome deficient *Arabidopsis* mutant *sse1* exhibits impaired fatty acid synthesis. *Plant Physiol.* **135**, 814–827
32. Kubota, H., Hynes, G., and Willison, K. (1995) The eighth Cct gene, Cctq, encoding the θ subunit of the cytosolic chaperonin containing TCP-1. *Gene* **154**, 231–236
33. Valpuesta, J. M., Martín-Benito, J., Gómez-Puertas, P., Carrascosa, J. L., and Willison, K. R. (2002) Structure and function of a protein folding machine. The eukaryotic cytosolic chaperonin CCT. *FEBS Lett.* **529**, 11–16
34. Yi, C., Li, S., Wang, J., Wei, N., and Deng, X. W. (2006) Affinity purification reveals the association of WD40 protein constitutive photomorphogenic 1 with the hetero-oligomeric TCP-1 chaperonin complex in mammalian cells. *Int. J. Biochem. Cell Biol.* **38**, 1076–1083
35. Zheng, H., Camacho, L., Wee, E., Batoko, H., Legen, J., Leaver, C. J., Malhó, R., Hussey, P. J., and Moore, I. (2005) A Rab-E GTPase mutant acts downstream of the Rab-D subclass in biosynthetic membrane traffic to the plasma membrane in tobacco leaf epidermis. *Plant Cell* **17**, 2020–2036
36. Bourne, H. R., Sanders, D. A., and McCormick, F. (1991) The GTPase superfamily. Conserved structure and molecular mechanism. *Nature* **349**, 117–127
37. Hayashi, M., Toriyama, K., Kondo, M., and Nishimura, M. (1998) 2,4-Dichlorophenoxybutyric acid-resistant mutants of *Arabidopsis* have defects in glyoxysomal fatty acid β -oxidation. *Plant Cell* **10**, 183–195
38. Zolman, B. K., Yoder, A., and Bartel, B. (2000) Genetic analysis of indole-3-butyric acid responses in *Arabidopsis thaliana* reveals four mutant classes. *Genetics* **156**, 1323–1337
39. Mukai, S., Ghaedi, K., and Fujiki, Y. (2002) Intracellular localization, function, and dysfunction of the peroxisome-targeting signal type 2 receptor, Pex7p, in mammalian cells. *J. Biol. Chem.* **277**, 9548–9561
40. Nair, D. M., Purdue, P. E., and Lazarow, P. B. (2004) Pex7p translocates in and out of peroxisomes in *Saccharomyces cerevisiae*. *J. Cell Biol.* **167**, 599–604
41. Purdue, P. E., and Lazarow, P. B. (2001) Pex18p is constitutively degraded during peroxisome biogenesis. *J. Biol. Chem.* **276**, 47684–47689
42. Anthonio, E. A., Brees, C., Baumgart-Vogt, E., Hongu, T., Huybrechts, S. J., Van Dijck, P., Mannaerts, G. P., Kanaho, Y., Van Veldhoven, P. P., and Fransen, M. (2009) Small G proteins in peroxisome biogenesis. The potential involvement of ADP-ribosylation factor 6. *BMC Cell Biol.* **10**, 58
43. Schollenberger, L., Gronemeyer, T., Huber, C. M., Lay, D., Wiese, S., Meyer, H. E., Warscheid, B., Saffrich, R., Peränen, J., Gorgas, K., and Just, W. W. (2010) RhoA regulates peroxisome association to microtubules and the actin cytoskeleton. *PLoS One* **5**, e13886
44. Rutherford, S., and Moore, I. (2002) The *Arabidopsis* Rab GTPase family. Another enigma variation. *Curr. Opin. Plant Biol.* **5**, 518–528
45. Woollard, A. A., and Moore, I. (2008) The functions of Rab GTPases in plant membrane traffic. *Curr. Opin. Plant Biol.* **11**, 610–619
46. Zhang, J. W., and Lazarow, P. B. (1995) PEB1 (PAS7) in *Saccharomyces cerevisiae* encodes a hydrophilic, intra-peroxisomal protein that is a member of the WD repeat family and is essential for the import of thiolase into peroxisomes. *J. Cell Biol.* **129**, 65–80
47. Ghys, K., Fransen, M., Mannaerts, G. P., and Van Veldhoven, P. P. (2002) Functional studies on human Pex7p. Subcellular localization and interaction with proteins containing a peroxisome-targeting signal type 2 and other peroxins. *Biochem. J.* **365**, 41–50
48. Dodt, G., and Gould, S. J. (1996) Multiple PEX genes are required for proper subcellular distribution and stability of Pex5p, the PTS1 receptor. Evidence that PTS1 protein import is mediated by a cycling receptor. *J. Cell Biol.* **135**, 1763–1774
49. Yahraus, T., Braverman, N., Dodt, G., Kalish, J. E., Morrell, J. C., Moser, H. W., Valle, D., and Gould, S. J. (1996) The peroxisome biogenesis disorder group 4 gene, PXAAA1, encodes cytoplasmic ATPase required for stability of the PTS1 receptor. *EMBO J.* **15**, 2914–2923
50. Ling, Q., Huang, W., Baldwin, A., and Jarvis, P. (2012) Chloroplast biogenesis is regulated by direct action of the ubiquitin-proteasome system. *Science* **338**, 655–659